# Optimized Space Vector Modulation for DC-Link Balancing in Three-Level Neutral-Point-Clamped Inverters for Electric Drives

Michael Laumen, Michael Schubert, Andreas Bubert, Alexander Lamprecht and Rik W. De Doncker
Institute for Power Electronics and Electrical Drives (ISEA) – RWTH Aachen University
Jägerstraße 17/19 – 52066 Aachen – Germany
Email: post@isea.rwth-aachen.de

***Abstract*—Multilevel inverters can replace conventional two-level inverters in many applications, as they offer less harmonic distortion on the output voltage and reduce losses in certain cases. Especially in electric vehicle traction applications, multilevel inverters can improve the system efficiency significantly and increase the cruising range. A popular topology is the three-level neutral-point-clamped (NPC) inverter. However, in contrast to conventional two-level converters, a low frequency ripple on the midpoint of the dc-link capacitors can occur.**

**In this paper, an optimized space vector modulation (SVM) scheme for dc-link balancing based on a combination of nearest three vector SVM and radial state SVM is introduced. The presented modulation scheme ensures a low voltage ripple on the midpoint of the dc-link over a wide operating range. Additionally, static voltage deviations can be eliminated to obtain a fully balanced dc-link. Simulation results of the proposed modulation scheme are presented for the entire operating range of a 160 kW induction machine. The performance is evaluated by a comparison with other modulation schemes.**

## I. Introduction

Electric vehicles are gaining more and more interest as they are a major part on the way to reduce air pollution, especially in metropolitan areas. Although costs for the batteries are dropping, they are still the main cost driver of electric vehicles. Therefore, a high efficiency is critical to achieve a sufficient cruising range at reasonable system cost.

High voltage induction machines offer lower currents, therefore the wire cross section and the weight can be reduced significantly. Using three-level neutral-point-clamped (NPC) inverters instead of conventional two-level converters reduces total harmonic distortions as well as losses significantly [1], [2]. Additionally, for a dc-link voltage of, e.g., 800 V, automotive qualified semiconductors with blocking voltages of 650 V can be used. These semiconductors offer lower switching losses, which results in a higher efficiency.

However, in an NPC inverter special care should be taken with respect to the dc-link capacitor. Besides the high frequency ripple induced by the switching of the semiconductors, a low frequency ripple with a frequency which three times higher than the output fundamental frequency can occur. Additionally, a static deviation of the midpoint voltage can appear, e.g., due to an unbalanced output of the inverter during speed-up of the induction machine. When using space vector modulation (SVM) [3], direct control of the switching states is possible compared to common sine triangle pulse width modulation (PWM), thus the midpoint voltage can be controlled.

The origin of the unbalanced midpoint currents and several methods for compensation of these currents were proposed in literature. In [4] and [5], it is shown how the redundancy of low voltage and high voltage switching states can be utilized to reduce the midpoint current for low output voltages. Another modulation scheme for higher voltages has been introduced in [6]. It eliminates the ripple by avoiding certain vectors which cause a midpoint current. As this reduces the possible switching states, additional harmonics occur in the output voltage and can cause more losses in the machine. Recently, a new modulation scheme to reduce the midpoint current while decreasing losses was presented [7], but an active neutral-point-clamped (ANPC) inverter was used, which requires additional switches compared to an NPC converter.

In this paper, the conventional nearest three vectors (NTV) SVM and radial state space vector modulation (RSS) are compared and an optimized modulation strategy is derived. Depending on the output currents and the modulation index, different methods are used to reduce or eliminate the ac ripple. Furthermore, steady state errors on the dc-link voltage can be compensated and an arbitrary midpoint current can be set.

First, the simulation environment and the topology is introduced. The NTV as well as the RSS modulation schemes are investigated with regard to the dc-link voltage. To show influences of the modulation scheme on the losses and on loss sharing between the semiconductors, the losses are analyzed on a per switch basis. In a next step an optimized modulation strategy is derived. Simulation results are presented to validate the effect on the dc-link and the influences on the inverter losses.

## II. Inverter Topology

The topology of the considered traction drive is shown in Fig. 1. It consists of an induction machine and a three-level NPC inverter connected to an 800 V battery pack.

The inverter has a maximum output power of 160 kW at a dc-link voltage of 800 V. Three single-phase three-level NPC modules *SKM300MLI066TAT* from *Semikron* are used.

978-1-5090-2364-6/17/$31.00 ©2017 IEEE

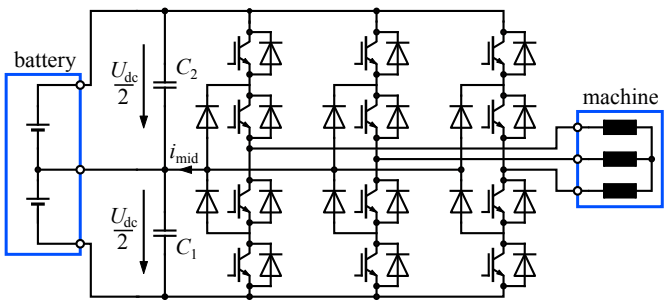


Fig. 1. Topology of the three-phase drive system with three-level NPC inverter.

The NPC topology offers the three different output voltages $-U_{dc}/2$, $U_{dc}/2$ and 0.

The dc-link is equipped with two 700 µF foil capacitors in series configuration.

A three-phase induction machine with a maximum torque of 250 Nm and a maximum speed of 15 000 rpm is utilized. Currents of up to 225 A and a power factor in the range of 0.62 to 0.97 are expected.

The battery consists of two series connected standard automotive rated battery packs with a voltage of 400 V each. To allow a limp-home feature the midpoint of the battery is connected to the midpoint of the dc-link. Thereby, the low frequency current ripple of the neutral point propagates to the battery, damped by the LC-filter, which consists of parasitic line inductances and the dc-link capacitor. This produces additional losses within the battery and may accelerate the ageing of the cells [8].

### A. Simulation

Simulations have been carried out in MATLAB Simulink with PLECS Blockset. Parameters that are obtained from datasheet curves of the switching behavior are used in PLECS to calculate detailed switching and conduction losses for the switches and the diodes. Additional losses, e.g., resistive losses in cables or connections, are not considered in the simulation.

For better illustration, the connection of the midpoint between the battery stack and the dc-link capacitors is not considered in the simulation model because it decreases the voltage ripple and distorts the results depending on the size of the parasitic line inductance and the inner resistance of the battery. Instead, ideal capacitors are used with a floating midpoint, so that the midpoint current will directly influence the voltage.

## III. Space Vector Modulation Schemes

The vectors of three-level SVM are grouped into zero, small, medium and large vectors depending on the length and the impact on the neutral-point balance [5]. A diagram of all possible switching states is depicted in Fig. 2. The triangles of the space vector diagram can be subdivided into four regions which are highlighted by different colors in Fig. 2.

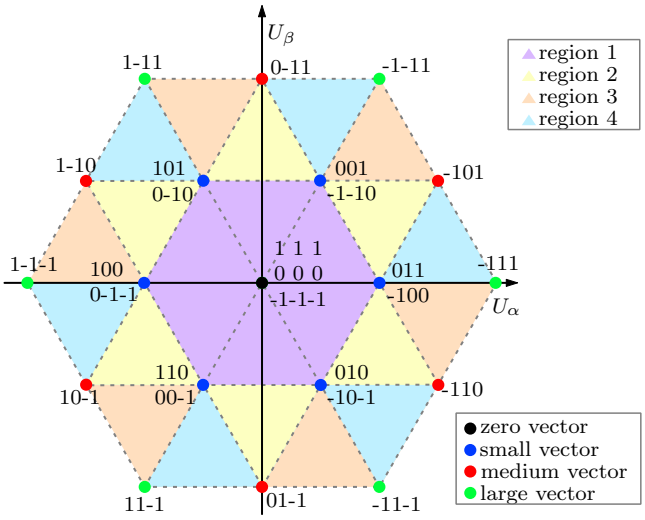


Fig. 2. Space vector diagram for three-level NPC inverters.

For the zero vectors all three half-bridges are in the same switching state of either -1 ($-U_{dc}/2$), 0 or 1 ($U_{dc}/2$). For states -1 and 1 no phase is connected to the midpoint and no midpoint current $i_{mid}$ flows. The same applies for state 0, where all phases are connected to the midpoint. The sum of the currents in this three-phase systems then equals zero. Therefore, it is not required to consider these vectors when calculating the neutral point current.

Consequently, also large vectors will not lead to a midpoint current as in this case no phase is connected to the midpoint.

Small vectors affect the midpoint in a controllable way, because they come in pairs of the same output voltages but opposite midpoint current direction where either one phase is connected to the midpoint or the other two.

Medium vectors induce switching states with non-controllable midpoint current since no alternative switching state with equal output voltage exists.

## IV. Comparison of SVM Schemes

In this section, common modulation schemes known from literature are introduced and compared. The investigation focusses on the influence of the modulation schemes on the balance of the dc-link capacitor. Simulations have been carried out for the entire operating range of the induction motor drive.

A further detailed analysis of the loss distribution among the switches was done for selected operating points where significant differences between the analyzed modulation schemes occur.

### A. Nearest Three Vectors Modulation

NTV modulation is a conventional SVM scheme applicable for two- and three-level inverters. To synthesize a target voltage within the $\alpha\beta$-plane, the nearest three vectors of the triangle where the voltage vector is pointing to, are selected. The switching pattern for each reference space vector is calculated based on a linear combination of the selected

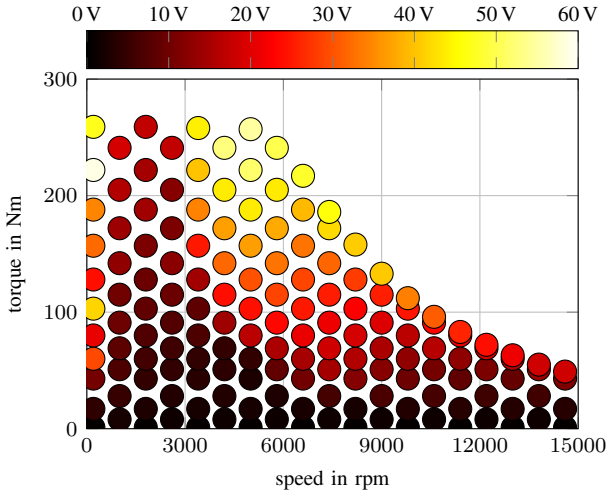


Fig. 3. Peak-to-peak voltage ripple of the capacitor midpoint for NTV modulation.

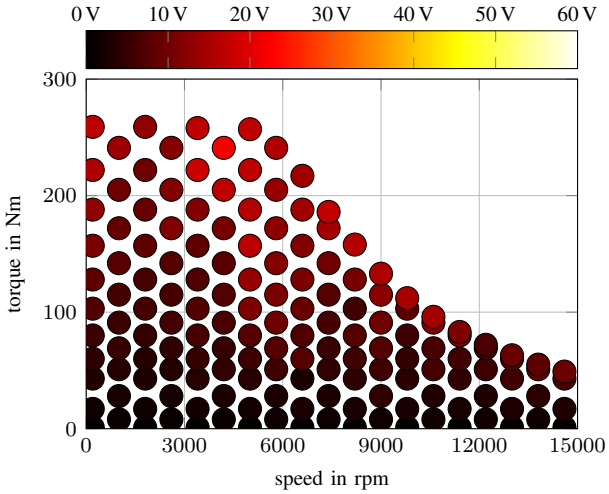


Fig. 4. Peak-to-peak voltage ripple of the capacitor midpoint for RSS modulation.

switching state vectors. For redundant switching state vectors (zero and small vectors) an equal distribution of the on-time is used to evenly distribute losses between the switches.

### *B. Radial State Space Modulation*

Medium vectors have a strong impact on the balance of the neutral point as they lead to a non-zero current $i_{\mathrm{mid}}$ with a frequency three times higher than the fundamental frequency of the output voltage. Therefore, RSS avoids the usage of medium vectors. If a switching sequence would require a medium vector, the two nearest large vectors are used instead. Thus, the current flow in the midpoint of the dc-link is eliminated. This leads to a total of four vectors instead of three which synthesize the reference voltage, and thus to a higher complexity of the modulator. Since certain switching states are avoided, a higher total harmonic distortion can be observed and additional losses in the induction machine will occur.

If only output voltages in region 1 are synthesized, the switching sequence contains no medium vector and thus RSS can't be applied. Other modulation schemes, e.g., NTV modulation, can be used instead.

Simulation results for the peak-to-peak value of the midpoint voltage are depicted in Fig. 4. Major differences can be observed when comparing the results with those of the NTV modulation in Fig. 3 or balanced NTV in Fig. 5. The maximum peak-to-peak voltage ripple could be reduced to 25 V.

### *C. Neutral-Point Balanced Nearest Three Vectors*

Balanced NTV is based on the principle of standard NTV modulation, but the redundancies of small vectors are used to reduce the current into the midpoint. Different methods can be used to scale the respective switching time. For example, a hysteresis controller [9] can switch between the two redundant vectors depending on the voltage offset of the capacitor. While reducing the third harmonic, this method has the disadvantage

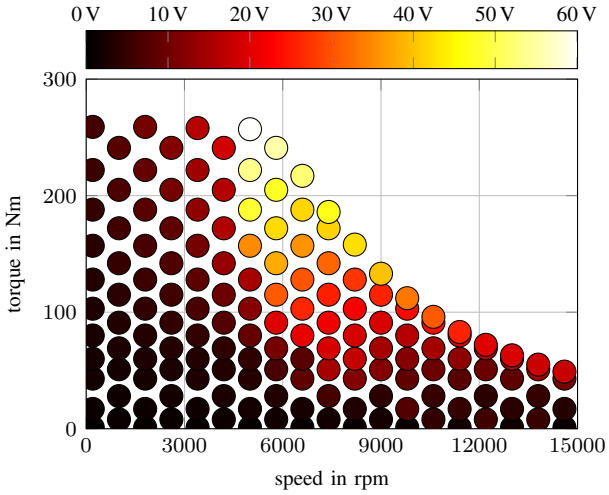


Fig. 5. Peak-to-peak voltage ripple of the capacitor midpoint for balanced NTV modulation.

of introducing a ripple of half the modulation frequency. Another approach utilizes a PI-controller to counteract on static deviations on the midpoint by adding an offset to the reference vector [4]. As the control is based on voltage measurements, a delay is unavoidable, which limits the effectiveness of this modulation scheme. Another modulation scheme based on midpoint current calculation is presented in [5], but this scheme leads to higher switching losses due to additional switching states and lesser robustness of the control.

## V. Neutral-Point Optimized SVM

Most of the modulation schemes presented in literature use a voltage measurement at the midpoint of the capacitor to identify static or dynamic deviations of the voltage. Due to delays in measurement and processing, a difference between the momentary voltage and the measurement result persists, which can lead to inaccurate balancing.

The space vector modulation can be optimized by predicting the midpoint voltage deviation at the end of the modulation period. Thereby, the charge difference between the two dc-link capacitors can be minimized and, consequently, the voltage ripple at the neutral point can be kept as low as possible. For the prediction, it is essential to know the midpoint current. Current sensors for the three-phase output of the inverter are often available due to the need for a robust control of the connected induction machine. They can be used to calculate $i_{\mathrm{mid}}$ instead of using a dedicated current sensor. The current $i_{\mathrm{mid}}$ induced by a single switching vector can be calculated by taking the switching state $s_n$ (0, -1 or 1) and the phase current $I_n$, which is considered as constant within the switching state, of each phase into account, where $n$ denotes the phase number:

$$i_{\mathrm{mid}} = -\sum_{n=1}^{3} I_n \cdot (1 - |s_n|) \tag{1}$$

To get the charge differences of the capacitors, in a first step, the switching patterns for conventional space vector modulation are generated. Next, the charge difference caused by switching states of medium vectors is calculated for one modulation period by considering the midpoint current $i_{\mathrm{mid}}$ and the on-time of each state.

As only switching states containing a medium vector contribute to a non-controllable midpoint current, calculation of the charge difference for the other states can be omitted. Taking the on-time $t_{\mathrm{on,med}}$ of the medium vector and the midpoint current $i_{\mathrm{mid}}$ into account, the charge difference $Q_{\mathrm{diff,med}}$ induced by the medium vector within a modulation period can be calculated to:

$$Q_{\mathrm{diff,med}} = t_{\mathrm{on,med}} \cdot i_{\mathrm{mid,m}}$$

The current $i_{\mathrm{mid}}$ is considered as constant within each modulation period to simplify the calculation. The simplification is valid when the modulation frequency is much higher than the fundamental output frequency, as the current then does not change much during one modulation period.

Using the redundancy of the small vectors, the charge $Q_{\mathrm{diff,med}}$ can be reduced or even fully compensated by the usage of redundant pairs of small vectors. Since the total on-time of the small vectors cannot be altered, a sharing factor $x$ is introduced to divide the on-time between a pair of redundant switching states. Either two pairs (region 1 and 2) or one pair of small vectors (region 3 and 4) is used to synthesize the voltage depending on the region of the reference voltage vector.

For region 3 and 4 the range of the charge difference $Q_{\mathrm{diff,small}}$ caused by the small vectors with on-time $t_{\mathrm{on,small}}$ is given by:

$$Q_{\mathrm{diff,small}} = t_{\mathrm{on,small}} \cdot (x \cdot i_{\mathrm{mid,s}} + (2 - x) \cdot i_{\mathrm{mid,s^*}}) \tag{2}$$

The currents $i_{\mathrm{mid,s}}$ and $i_{\mathrm{mid,s^*}}$ represent the midpoint current induced by the pair of small vectors. As both vectors create the same output voltage but connect opposite phases to the midpoint, for a symmetric three-phase system the relation $i_{\mathrm{mid,s}} = -i_{\mathrm{mid,s^*}}$ is used to further simplify equation (2):

$$Q_{\mathrm{diff,small}} = 2 \cdot t_{\mathrm{on,small}} \cdot i_{\mathrm{mid,s}} \cdot (x - 1) \tag{3}$$

To get the value of $x$ where the charge induced by the medium vectors is fully compensated, equation (3) must be solved for $x$ with $Q_{\mathrm{diff,small}} = -Q_{\mathrm{diff,med}}$:

$$x = 1 - \frac{Q_{\mathrm{diff,med}}}{2 \cdot t_{\mathrm{on,small}} \cdot i_{\mathrm{mid,s}}} \tag{4}$$

The switching times of both vectors of the pair of redundant small vectors are now scaled with $x$ and $(2 - x)$, respectively.

Depending on the output voltage, it might not be possible to perfectly compensate the charge, as the time $t_{\mathrm{on,small}}$ and, consequently the charge $Q_{\mathrm{diff,small}}$ decreases for a high modulation index. In this case, the value of $x$ according to equation (4) would be outside of the allowed bounds of 0 and 2. Instead of limiting the value and thereby getting an incomplete compensation, the initial switching patterns are replaced by those of radial state space vector modulation, whereby the medium vector is avoided.

For region 1 and 2 of the space vector diagram two pairs of redundant small vectors can be used to compensate the charge difference. Analog to equation (3), the charge can be calculated taking the additional midpoint currents of the second vector pair $i_{\mathrm{mid,s2}}$ and $i_{\mathrm{mid,s2^*}}$ as well as the on-time $t_{\mathrm{on,small2}}$ into account. To simplify the calculation, equal sharing factors are used for both vector pairs.

$$\begin{aligned} Q_{\mathrm{diff,small}} = {} & 2 \cdot t_{\mathrm{on,small}} \cdot i_{\mathrm{mid,s}} \, (x - 1) \\ & + 2 \cdot t_{\mathrm{on,small2}} \cdot i_{\mathrm{mid,s2}} \cdot (x - 1) \end{aligned} \tag{5}$$

Solving equation (5) for $x$ analog to equation (4) leads to:

$$x = 1 - \frac{Q_{\mathrm{diff,med}}}{2 \cdot t_{\mathrm{on,small}} \cdot i_{\mathrm{mid,s}} + 2 \cdot t_{\mathrm{on,small2}} \cdot i_{\mathrm{mid,s2}}} \tag{6}$$

If the signs of $i_{\mathrm{mid,s}}$ and $i_{\mathrm{mid,s2}}$ differ from each other, $i_{\mathrm{mid,s2^*}}$ instead of $i_{\mathrm{mid,s2}}$ is used in the calculations of $Q_{\mathrm{diff,small}}$ (equation (5)) and $x$ (equation (6)).

Static voltage deviations can be further eliminated by calculating a charge offset in the first step based on the measured voltage imbalance of the dc-link capacitors. Given the midpoint voltage $-U_{\mathrm{dc}}/2$ and the capacitance $C_1$ of one part of the dc-link, the total charge difference is given by:

$$Q_{\mathrm{diff}} = Q_{\mathrm{diff,med}} + C_1 \cdot (U_{\mathrm{dc}}/2 - U_{\mathrm{ref}}) \tag{7}$$

The voltage reference $U_{\mathrm{ref}}$ is set to half of the dc-link voltage, but it can also be set to a time dependent voltage, e.g., to create an arbitrary voltage waveform at the midpoint of the dc-link.

Simulation results of the peak-to-peak dc-link midpoint voltage for the entire operating range of the induction machine are depicted in Fig. 7. In comparison to NTV and balanced NTV modulation in Fig. 3 and Fig. 5, respectively, the peak-to-peak voltage at the midpoint is drastically reduced from around 55 V to 20 V. When comparing to the simulation results for RSS in Fig. 4, only small differences can be noticed with regard to the peak-to-peak voltage. A major advantage of the

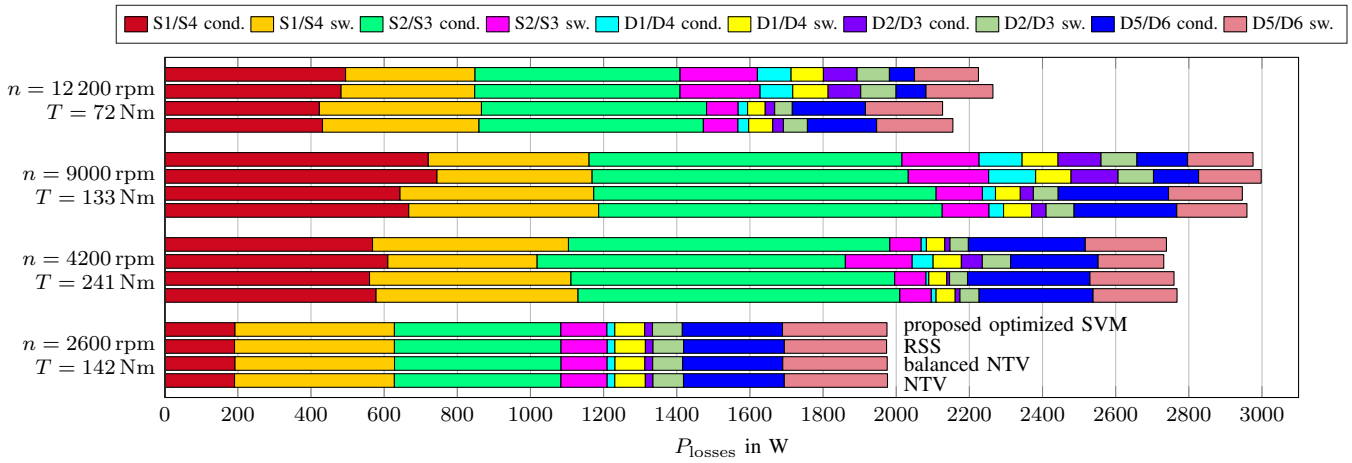


Fig. 6. Switching (sw.) and conduction (cond.) losses for different operating points and modulation schemes.

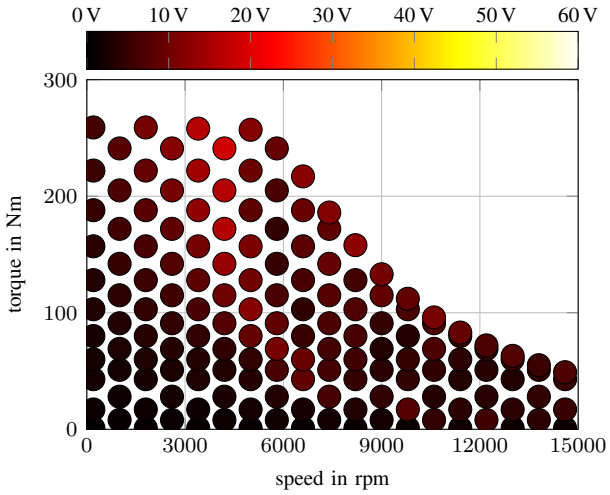


Fig. 7. Peak-to-peak voltage ripple of the capacitor midpoint for the neutral-point optimized SVM.

proposed scheme is the ability to balance the midpoint for static voltage differences, e.g., due to machine transients. In RSS modulation a static offset and thus unequal load sharing between the switches can occur.

For comparison of the total inverterlosses and the loss sharing among the switches and diodes, the switching and conduction losses of the switches $\mathrm{S}_1$ to $\mathrm{S}_4$, the corresponding diodes $\mathrm{D}_1$ to $\mathrm{D}_4$ and the clamping diodes $\mathrm{D}_5$ and $\mathrm{D}_6$ were simulated. When utilizing the proposed modulation, the inverter losses lie between the losses of NTV and RSS modulation.

Comparing the loss sharing between the switches, larger differences can be noticed. Switching losses of the inner switches $\mathrm{S}_2$ and $\mathrm{S}_3$ are slightly higher for RSS modulation compared to NTV modulation, while switching losses of the outer switches $\mathrm{S}_1$ and $\mathrm{S}_4$ are reduced at the same time. For lower output voltages (e.g., for $n = 2600\,{}^1/_{\mathrm{min}}$, $T = 142\,\mathrm{Nm}$), the optimized SVM shows a similar loss sharing than NTV, $T = 142\,\mathrm{Nm}$), for higher output voltages the optimized SVM shows a similar behavior as RSS modulation.

## VI. Conclusions

A dc-link voltage ripple optimized space vector modulation for NPC inverters showing lower peak-to-peak voltages has been introduced. Simulation results for the entire operating range of a 160 kW electric vehicle induction machine were presented. The results prove, that the maximum peak-to-peak voltage could be reduced to 20 V, including the high frequency voltage ripple due to the switching of the semiconductors. Thus, a reduction of around 35 V in comparison to conventional modulation schemes could be achieved.

The loss sharing among the inverter switches for the different modulation schemes has been compared. Depending on the output voltage, the distribution of the losses among the switches for the optimized SVM are either comparable to those of NTV (for lower output voltage) or to those of RSS modulation (for higher output voltage).

An analysis of the total inverter losses has been carried out. It has been shown that the performance of the presented modulation is better than RSS, but for some operating points slightly worse than NTV. As a lower midpoint voltage ripple as well as a better efficiency cannot be reached at the same time, the proposed modulation scheme is a good trade-off between NTV and RSS.

## Acknowledgment

The work for this paper has been carried out within the research project H3Top, which is funded by the German Federal Ministry of Education and Research (BMBF, support code 16EMO0176).

## References

[1] A. Nabae, I. Takahashi, and H. Akagi, “A New Neutral-Point-Clamped PWM Inverter,” *IEEE Transactions on Industry Applications*, vol. IA-17, no. 5, pp. 518–523, Sep. 1981.

[2] A. Bubert, S.-H. Lim, and R. W. De Doncker, "Comparison of B6C and NPC Inverter Topologies for Electric Vehicle Application," *IEEE Southern Power Electronics Conference (SPEC)*, 2017, Submitted for peer-review.

[3] H. W. van der Broeck, H. C. Skudelny, and G. V. Stanke, "Analysis and realization of a pulsewidth modulator based on voltage space vectors," *IEEE Transactions on Industry Applications*, vol. 24, no. 1, pp. 142–150, Jan. 1988, ISSN: 0093-9994.

[4] C. Newton and M. Sumner, "Neutral point control for multi-level inverters: theory, design and operational limitations," in *Conference Record of the IEEE Thirty-Second IAS Annual Meeting*, vol. 2, Oct. 1997, pp. 1336–1343.

[5] N. Celanovic and D. Boroyevich, "A comprehensive study of neutral-point voltage balancing problem in three-level neutral-point-clamped voltage source PWM inverters," *IEEE Transactions on Power Electronics*, vol. 15, no. 2, pp. 242–249, Mar. 2000.

[6] A. Bendre and G. Venkataramanan, "Radial state space vector modulation-a new space vector technique for reducing DC link capacitor harmonic currents in three level converters," in *38th IAS Annual Meeting on Conference Record of the Industry Applications Conference*, vol. 1, Oct. 2003, 684–691 vol.1.

[7] C. Hu, X. Yu, D. G. Holmes, W. Shen, Q. Wang, F. Luo, and N. Liu, "An Improved Virtual Space Vector Modulation Scheme for Three-Level Active Neutral-Point-Clamped Inverter," *IEEE Transactions on Power Electronics*, vol. 32, no. 10, pp. 7419–7434, Oct. 2017.

[8] S. Y. Cho, I. O. Lee, J. I. Baek, and G. W. Moon, "Battery Impedance Analysis Considering DC Component in Sinusoidal Ripple-Current Charging," *IEEE Transactions on Industrial Electronics*, vol. 63, no. 3, pp. 1561–1573, Mar. 2016.

[9] R. Rojas, T. Ohnishi, and T. Suzuki, "An improved voltage vector control method for neutral-point-clamped inverters," *IEEE Transactions on Power Electronics*, vol. 10, no. 6, pp. 666–672, Nov. 1995.